Journal of Molecular Catalysis A: Chemical 356 (2012) 152–157

Contents lists available at SciVerse ScienceDirect

Journal of Molecular Catalysis A: Chemical

journal homepage: www.elsevier.com/locate/molcata

An antimony(V) substituted Keggin heteropolyacid, $H_4PSbMo_{11}O_{40}$: Why is its catalytic activity in oxidation reactions so different from that of $H_4PVMo_{11}O_{40}$?

Hila Goldberg[a], Devesh Kumar[b,1], G. Narahari Sastry[b], Gregory Leitus[c], Ronny Neumann[a,*]

[a] Department of Organic Chemistry, Weizmann Institute of Science, Rehovot 76100, Israel
[b] Molecular Modeling Group, Indian Institute of Chemical Technology, Hyderabad 500 607, India
[c] Chemical Research Support Unit, Weizmann Institute of Science, Rehovot 76100, Israel

ARTICLE INFO

Article history:
Received 16 August 2011
Received in revised form
19 December 2011
Accepted 21 December 2011
Available online 18 January 2012

Keywords:
Polyoxometalate
Antimony
Molybdenum
Oxidation
DFT

ABSTRACT

An antimony(V) containing α-Keggin type *acidic* polyoxometalate, $H_4PSbMo_{11}O_{40}$, was prepared by reacting $NaMoO_4$, H_3PO_4 and Sb_2O_3 in the presence of aqua regia to appraise its reactivity compared to the well known vanadate analog, $H_4PVMo_{11}O_{40}$. Characterization was by X-ray diffraction, MALDI-TOF MS, IR, UV–vis and ^{31}P NMR spectroscopy. Catalytic redox reactions, such as oxidative dehydrogenation using O_2 and N_2O as terminal oxidants were studied and showed very different reactivity of $H_4PSbMo_{11}O_{40}$ versus $H_4PVMo_{11}O_{40}$. It was found by DFT calculations that in contrast to analogous $H_4PVMo_{11}O_{40}$ where vanadium centered catalysis is observed, in $H_4PSbMo_{11}O_{40}$ catalysis is molybdenum and not antimony centered.

1. Introduction

Polyoxometalates exhibit a variety of structures and properties that make them useful in catalysis, material science and medicine [1]. They can be viewed as polyanions of discrete structure composed of mixtures of metal oxides containing both main group and transition metal elements. Our interest in polyoxometalates has been as liquid phase homogeneous catalysts, but heterogeneous, gas phase oxidation catalysis is also an important area of research [2]. The catalytic activity and reaction selectivity in polyoxometalate catalyzed reactions is dependent on many parameters most notably the elemental composition. Equally important are the overall structure, acidity and/or counter cation, and charge and within the polyoxometalate structure. Specifically, *acidic* phosphovanadomolybdates, $H_{3+x}PV_xMo_{12-x}O_{40}$ where $x = 1$, 2, but especially $x = 2$ show interesting redox activity that can be translated to oxidation and oxygenation of organic substrates by electron transfer and electron transfer–oxygen transfer mechanisms as reported extensively by us [3,4]. Importantly the reduced catalyst can be conveniently reoxidized with dioxygen under mild conditions even though they are stable also at significantly higher temperatures [3,4].

Antimony oxides are well-known components of heterogeneous oxidation catalysts, such as $VSbO_4$ for propane ammonoxidation, alkylaromatic ammonoxidation and in allylic oxidations [24]. It is also known that antimony in the secondary structure of polyoxometalates as counter cations have a stabilizing effect on polyoxometalates at high temperatures (>400 °C) [25]. There are quite a significant number of polyoxomolybdates and polyoxotungstates reported in the literature containing Sb(III) atoms, where the lone pair on Sb occupies a coordination position and the compounds are non-acidic, that is they are not heteropolyacids [26–44]. Most of these studies are based on structural aspects with only sparse use in catalysis. Our search of the literature has revealed only five Sb(V) containing compounds [45–49]. In this context it should be emphasized that we have reported on the tetrabutyl ammonium salt of $[PSb(V)Mo_{11}O_{40}]^{4-}$ via oxidation of an antimony(III) compound with ozone but an antimony(V) containing Keggin *heteropolyacid* has not been disclosed. The distinction is important for only the acids are reactive in electron transfer (ET) and electron transfer–oxygen transfer (ET–OT) reactions [3–23].

In this research we were interested in probing the question on how the replacement of vanadium(V) in $H_{3+x}PV_xMo_{12-x}O_{40}$ by antimony(V) to yield the similar $H_{3+x}PSb_xMo_{12-x}O_{40}$ compounds would effect the catalytic activity in electron transfer and electron transfer–oxygen transfer type reactions? [3] Differences were

* Corresponding author. Tel.: +972 8 934 3354; fax: +972 8 934 4142.
E-mail address: Ronny.Neumann@weizmann.ac.il (R. Neumann).
[1] Present address: Department of Applied Physics, School for Physical Sciences, Babasaheb Bhimrao Ambedkar University, Vidya Vihar, Rae Bareilly Road, Lucknow (U.P.) 226 025, India.

1381-1169/$ – see front matter © 2012 Elsevier B.V. All rights reserved.
doi:10.1016/j.molcata.2011.12.033

Table 1
Crystallographic Data for $H_4PSbMo_{11}O_{40}\cdot 14H_2O$.

Empirical formula	$PSb_1Mo_{11}O_{40}+14O$
Molecular weight	2072.06
Crystal system	Triclinic
Space group	$P\bar{1}$
a, Å	13.602(3)
b, Å	13.944(2)
c, Å	13.946(3)
α,°	60.72(3)
β,°	68.44(3)
γ,°	70.50(2)
Volume, Å^3; Z	2106.7(10); 2
Density$_{calc}$, mg cm^{-1}	3.267
μ, mm^{-1}	3.962
Reflections	33,799
Unique reflections	11,289
R_{int}	0.0224
R_1; wR_2 ($I>2\sigma(I)$)[a]	0.0307; 0.0697
R_1; wR_2 (all data)[a]	0.0377; 0.0730

[a] $R_1=\sum||F_o|-|F_c||/\sum|F_o|$; $wR_2=\{\sum[w(F_o^2-F_c^2)^2]/\sum w(F_o^2)^2\}^{1/2}$.

expected for a number of reasons: (1) The common oxidation states of vanadium in polyoxometalates are 4+ and 5+, whereas for antimony typically 3+ and 5+ oxidation states have been observed. This could conceivably lead to a one-step two-electron oxidation of substrates with $H_{3+x}PSb_xMo_{12-x}O_{40}$ versus two consecutive one-electron oxidations commonly observed for $H_{3+x}PV_xMo_{12x}O_{40}$. (2) The significantly higher electronegativity of antimony versus vanadium should render the neighboring oxygen atoms more electropositive and in this way could conceivably improve the oxygen donation reactivity of $H_{3+x}PSb_xMo_{12-x}O_{40}$.

2. Results and discussion

The synthesis of $H_{3+x}PSb_xMo_{12-x}O_{40}$ for $x=1$ and 2 was carried out in the typical manner for such polyoxometalates [50] which involves the reaction of the required stoichiometric amounts of phosphate, antimonate and molybdate under acidic conditions. The major difference vis-a-vis the analogous $H_{3+x}PV_xMo_{12-x}O_{40}$ synthesis was to prepare the antimony(V) precursor in situ by oxidation of Sb_2O_3 with aqua regia. Extraction with ether and recrystallization of $H_4PSbMo_{11}O_{40}$ was successful while the synthesis of $H_5PSb_2Mo_{10}O_{40}$ was not due to insufficient stability of the product obtained. Subsequent research was on $H_4PSbMo_{11}O_{40}$ only. It should be noted that a different procedure used in the past using Sb_2O_5 as antimony(V) precursor failed [35].

$H_4PSbMo_{11}O_{40}$ crystallized in the triclinic space group *P-1* with two slightly different α-Keggin moieties per asymmetric unit. For details of the structural analysis, see Table 1, Section 4, and the cif file in the Supporting Information. Generally, in most mono-substituted α-Keggin structures the substituted metal atom positions are fully disordered due to the cubic crystal structure [51]. Here, the lower triclinic symmetry has allowed us to determine that when the compound crystallizes it showed a Sb content of 1.02 Sb atoms (also observed in elemental analysis) per PMo(Sb)O cluster. The refinement when the sum of the Sb occupancies was fixed to be equal 1 gives an *R* factor of 0.0307 whereas when it was assumed that no Sb was incorporated the *R* factor was significantly higher, 0.052, Fig. 1. The Mo—O and Sb—O bonds lengths are typical for phosphomolybdates and not statistically different from each other that is, the Sb—O bonds lengths are within one standard deviation of those of the respective Mo—O bond lengths. It should be noted that 14 water molecules were located for each polyoxometalate unit. This amount of water was confirmed also by thermogravimetric analysis which showed a loss of 11.5% water at up to circa 100 °C.

The X-ray diffraction characterization of $H_4PSbMo_{11}O_{40}$ was complemented by further spectroscopic and electrochemical

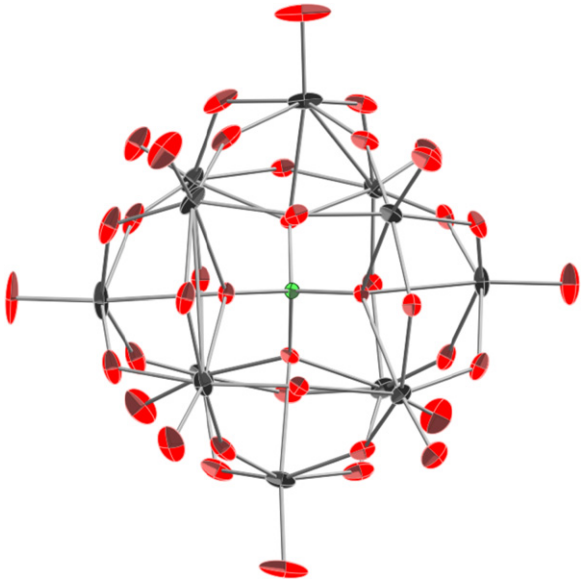

Fig. 1. ORTEP representation (50% probability) of $H_4PSbMo_{11}O_{40}\cdot 14H_2O$. Water molecules and protons not shown; P – green, Mo/Sb – black, O – red. (For interpretation of the references to color in this figure legend, the reader is referred to the web version of this article.)

characterization. The IR spectrum of $H_4PSbMo_{11}O_{40}$ has four peaks at 1064, 960, 869, and 781 cm^{-1} due to four different types of oxygen atoms (internal, edge shared, corner shared and terminal) and is typical for non-distorted α-Keggin structures of general T_d symmetry and essentially the same as the spectrum of $H_3PMo_{12}O_{40}$. A MALDI-TOF-MS of $H_4PSbMo_{11}O_{40}$ deposited from an acetonitrile solution showed a cluster of peaks at $m/z=1894.0540$ (90%) and 1771.0132 (100%) attributable to a protonated $H_4PSbMo_{11}O_{40}\cdot CH_3CN$ species and a lacunary species, respectively. No peak associable to the analogous $H_3PMo_{12}O_{40}$ compound was observed. The IR spectrum does not indicate the presence of a lacunary species in the sample itself that would lead to a split peak for the P—O vibration at 1064 cm^{-1} indicating that the lacunary species is formed as a metastable species upon ionization within the mass spectrometer. The ^{31}P NMR of $H_4PSbMo_{11}O_{40}$ has a single peak at $\delta=-2.298$ ppm, close to that of $H_3PMo_{12}O_{40}$ which has a peak at $\delta=-2.313$. The peaks, however, are *distinct* as shown by measuring the spectrum of a mixture of the two compounds. The cyclic voltammogram (1 mM $H_4PSbMo_{11}O_{40}$, 1 M $TBABF_4$ in CH_3CN) shows two reductions at 0.48 and 0.63 mV versus NHE.

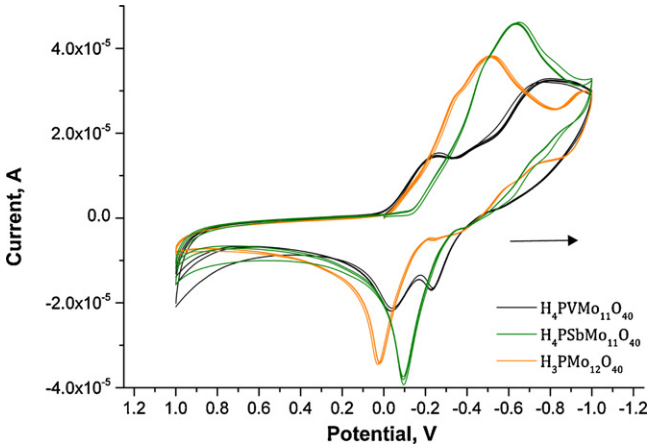

Fig. 2. Cyclic voltammograms of $H_4PSbMo_{11}O_{40}$ and $H_3PMo_{12}O_{40}$ (1 mM polyoxometalate, 1 M $(n\text{-}C_4H_9)_4NBF_4$ in CH_3CN, scan rate – 100 mV/s).

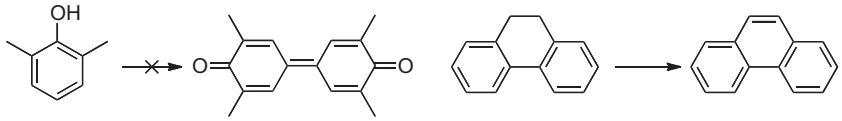

Scheme 1. Aerobic oxidation of 2,6-dimethyl phenol and dihydrophenanthrene catalyzed by $H_4PSbMo_{11}O_{40}$.

This is in contrast to the cyclic voltammogram of the $H_3PMo_{12}O_{40}$ "parent" polyoxometalate, which under identical conditions, also showed two reductions, however, at different and lower potentials, 0.33 and 0.48 mV versus NHE, Fig. 2. $H_4PSbMo_{11}O_{40}$ has a higher oxidation potential compared to $H_3PMo_{12}O_{40}$. $H_4PVMo_{11}O_{40}$ has oxidation potentials intermediate that of $H_4PSbMo_{11}O_{40}$ and $H_3PMo_{12}O_{40}$.

As mentioned in the introduction, we have shown that $H_{3+x}PV_xMo_{12-x}O_{40}$ is active in electron transfer (ET) and electron transfer–oxygen transfer (ET–OT) reactions. The reactions all begin by electron transfer from the organic substrate to the polyoxometalate to yield vanadium(IV) species. In ET only reactions there is no oxygen transfer from the catalyst to the activated substrate and the eventual product is a dehydrogenated compound. Examples include arenes from dihydroarenes [3,6], or diphenoquinones from phenols [5]. In ET–OT reactions, initial electron transfer is followed by oxygen transfer from the polyoxometalate to the activated substrate to yield oxygenated products. Examples include ketones and quinones from arenes and alkylarenes, respectively [9,10], the carbon—carbon bond cleavage in the oxidation of primary alcohols [19], and the oxygenation of sulfides [22]. We wished to gauge the reactivity of $H_4PSbMo_{11}O_{40}$ in both ET and ET–OT reactions.

In the presence of $H_4PVMo_{11}O_{40}$, 2,6-dimethyl phenol gives the corresponding diphenoquinone in quantitative yields through a four-electron oxidative dimerization reaction. In this reaction the corresponding $H_4PSbMo_{11}O_{40}$ showed no catalytic activity, Scheme 1. On the other hand, $H_4PSbMo_{11}O_{40}$ was reactive in electron transfer initiated oxidative dehydrogenations of dihydroarenes to arenes. For example, in Table 2, one can see the relative conversions using various catalysts and two oxidants for the oxidative dehydrogenation of dihydrophenanthrene to phenanthrene. In the aerobic oxidation, $H_4PSbMo_{11}O_{40}$ and $H_4PVMo_{11}O_{40}$ showed the same conversion after 15 h, while $H_3PMo_{12}O_{40}$ was significantly less reactive. The use of nitrous oxide as oxidant was also effective although the yields were significantly lower. It should be noted that in the absence of catalyst with both oxidants only trace amounts, ~1%, of dihydrophenanthrene were oxidized via a disproportionation pathway, that is reduced tetrahydro- and octahydrophenanthrene were also formed.

In order to differentiate more clearly between the catalytic activities of the various catalysts, the initial rates of the aerobic oxidative dehydrogenation of limonene to *para*-cymene were measured. This was done by observing the reduction of the polyoxometalate catalyst by UV–vis spectroscopy, through formation of the known reduced blue species at 700 nm. The relative reactivity was $H_4PVMo_{11}O_{40}$ (~20) > $H_4PSbMo_{11}O_{40}$ (~10) ≫ $H_3PMo_{12}O_{40}$ (1). Clearly, the antimony and vanadium substituted phosphomolybdates have similar activity for the aforementioned aromatization reactions that are in any case higher than that of the non-substituted compound. However, the scope of reactivity of $H_4PSbMo_{11}O_{40}$ was lower.

Table 2
Oxidative dehydrogenation of dihydrophenanthrene to phenanthrene.

Catalyst	Conversion, mol% O_2	Conversion, mol% N_2O
$H_4PSbMo_{11}O_{40}$	>99	26
$H_4PVMo_{11}O_{40}$	>99	24
$H_3PMo_{12}O_{40}$	31	25

Reaction conditions: dihydrophenanthrene (5 mmol), catalyst (0.5 mmol), acetic acid (1 mL), 1 bar O_2 or N_2O, 15 h, 110 °C. Conversions were measured by GC and no products besides phenanthrene were observed.

In contrast to $H_4PVMo_{11}O_{40}$ in ET–OT reactions no catalytic activity of $H_4PSbMo_{11}O_{40}$ was found for the oxygenation of active arenes and alkyl arenes such as anthracene and xanthene. Also no oxygenation of thioanisole with $H_4PSbMo_{11}O_{40}$ was observed. On the other hand for the oxidative carbon—carbon cleavage reaction of 1-butanol where phosphovanadomolybdates yielded *selective* 1:1 formation of butylformate and butylpropionate, the use of $H_4PSbMo_{11}O_{40}$ led to a mixture of products. Thus, oxidation of 1-butanol (1 mmol), $H_4PSbMo_{11}O_{40}$ (0.01 mmol), sulfolane (1 mL), 1 bar O_2 100 °C, 15 h, gave a low conversion of 1-butanol and a mixture of products, including the cleavage products, butylformate and butylpropionate, the autooxidation product, butanal, and the acid catalyzed etherification product, di-*n*-butylether, Scheme 2. The same reaction with $H_3PMo_{12}O_{40}$ gave *no* oxidation products and only di-*n*-butylether (17% yield). Clearly, $H_4PSbMo_{11}O_{40}$ was a significantly inferior catalyst for ET–OT reactions as compared to the analogous vanadium substituted compounds but did show some activity as opposed to $H_3PMo_{12}O_{40}$ which is totally inactive for such reactions. A post reaction measurement of the ^{31}P NMR spectrum of the reaction mixture showed no compounds except the original $H_4PSbMo_{11}O_{40}$ indicating that the catalyst was stable under reaction conditions.

In order to gain further insight into the potential of $H_4PSbMo_{11}O_{40}$ as an ET and ET–OT catalyst, calculations were carried out on $[PSbMo_{11}O_{40}]^{4-}$ to determine its energies and spin states using the same methodology previously used for the analogous $[PV_xMo_{12-x}O_{40}]^{(3+x)-}$ polyoxometalates [52]. Fig. 3 shows the numbering scheme used for the designation of the atoms in the calculations.

DFT calculations have been performed on all possible spin states and the stationary points have been characterized as minima on the potential energy surface. The two basis sets yielded essentially identical results and therefore the results are independent of basis set employed. However, the gas phase results were unable to provide any meaningful correlations with the observations. A cursory look at Tables 3–5 indicates the importance of calculations in solvent phase for corroboration with the observations. The two solvents employed, water and acetonitrile (ACN) yielded similar values. The following observations can be made from the systematic computational study: (1) For the fully oxidized compound $[PSbMo_{11}O_{40}]^{4-}$, the ground state is unambiguously characterized as a singlet. (2) All the compounds are expected to be low spin and only the one-electron reduced $[PSbMo_{11}O_{40}]^{5-}$ is expected to be paramagnetic with a doublet ground state; the oxidized and two-electron compounds are expected to be diamagnetic. (3) The one-electron reduced compound, $[PSbMo_{11}O_{40}]^{5-}$, is more

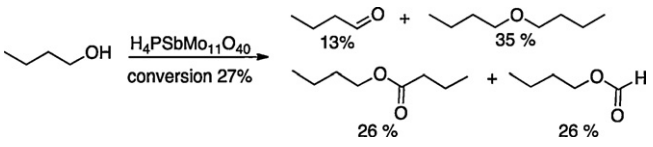

Scheme 2. Aerobic oxidation of 1-butanol catalyzed by $H_4PSbMo_{11}O_{40}$.

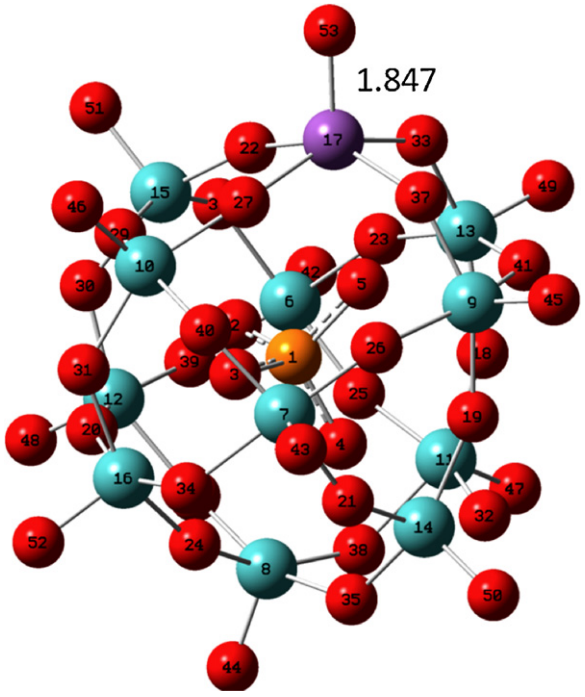

Fig. 3. The numbering scheme for the $[PSbMo_{11}O_{40}]^{q-}$ ($q = 4, 5, 6$) anion. Mo – blue, O – red, P – orange, Sb – purple. (For interpretation of the references to color in this figure legend, the reader is referred to the web version of this article.)

Table 3
B3LYP/B1 (top) and B3LYP/B2D//B1 (bottom) relative energies in kcal/mol for $^{1,3,5}[PSbMo_{11}O_{40}]^{4-}$.

	DE[a]			D(E+ZPC)[a]		
	Gas	Water	ACN	Gas	Water	ACN
M1	0.00	0.00	0.00	0.00	0.00	0.00
	0.00	0.00	0.00	0.00	0.00	0.00
M3	27.21	26.85	27.00	26.09	25.73	25.88
	36.14	35.78	35.93	35.02	34.66	34.81
M5	69.04	69.73	69.8	66.74	67.43	67.58
	88.51	89.20	89.35	86.21	86.90	87.05

[a] Values are with respect to $^{1}[PSbMo_{11}O_{40}]^{4-}$; M1 – singlet, M3 – triple, M5 – quintet, ACN – acetonitrile.

stable than the oxidized $[PSbMo_{11}O_{40}]^{4-}$ as may be expected for an oxidizing compound and the two-electron reduced compound, $[PSbMo_{11}O_{40}]^{6-}$, is yet more stable. The results support the electrochemical measurements and the positive oxidation potential of these compounds.

The B3LYP/B1 spin densities and charges (see ESI for the tables) for $^{1}[PSbMo_{11}O_{40}]^{4-}$, $^{2}[PSbMo_{11}O_{40}]^{5-}$, and $^{1}[PSbMo_{11}O_{40}]^{6-}$, shows that the charge on antimony remains unchanged over

Table 4
B3LYP/B1 (top) and B3LYP/B2D//B1 (bottom) relative energies in kcal/mol for $^{2,4,6}[PSbMo_{11}O_{40}]^{5-}$.

	DE[a]			D(E+ZPC)[a]		
	Gas	Water	ACN	Gas	Water	ACN
M2	128.83	−115.80	−111.41	127.66	−116.97	−112.58
	143.73	−100.90	−96.51	142.57	−102.06	−97.67
M4	172.17	−71.74	−67.46	169.57	−74.34	−70.06
	197.50	−46.41	−42.13	194.90	−49.01	−44.73
M6	211.01	−31.92	−27.54	207.53	−35.40	−31.02
	246.64	3.71	8.09	243.16	0.23	4.61

[a] Values are with respect to $^{1}[PSbMo_{11}O_{40}]^{4-}$; M2 – doublet, M4 – quartet, M6 – hextet.

Table 5
B3LYP/B1 (top) and B3LYP/B2D//B1 (bottom) relative energies in kcal/mol for $^{1,3,5}[PSbMo_{11}O_{40}]^{6-}$.

	DE[a]			D(E+ZPC)[a]		
	Gas	Water	ACN	Gas	Water	ACN
M1	327.08	−219.22	−208.70	324.85	−221.45	−210.93
	355.99	−190.31	−179.79	353.75	−192.55	−182.03
M3	324.18	−221.66	−211.11	321.45	−224.39	−213.84
	353.59	−192.25	−181.70	350.86	−194.98	−184.43
M5	364.84	−179.19	−168.67	360.83	−183.20	−172.68
	404.00	−140.03	−129.51	399.99	−144.04	−133.52

[a] Values are with respect to $^{1}[PSbMo_{11}O_{40}]^{4-}$; M1 – singlet, M3 – triple, M5 – quintet.

all three of the lowest energy states indicating that reduction *does not take place at the antimony atom.* Indeed, for the one-electron reduced $^{2}[PSbMo_{11}O_{40}]^{5-}$, the negative charge and spin density are mostly concentrated on the distal (to antimony) molybdenum atom, Mo14. Further, for the two-electron reduced $^{1}[PSbMo_{11}O_{40}]^{6-}$, the negative charge tends to be more delocalized over all molybdenum atoms with preference for Mo11 and Mo14. The calculations point out that although $H_4PSbMo_{11}O_{40}$ is isostructural to $H_4PVMo_{11}O_{40}$ and have similar ground state energies (−427.1 and −443.6 kcal/mol) the electronic ground states of the reduced compounds are very different. $H_4PVMo_{11}O_{40}$ shows vanadium-centered redox properties, whereas $H_4PSbMo_{11}O_{40}$ shows molybdenum-based redox chemistry. This indicates that $H_4PSbMo_{11}O_{40}$ is more similar to $H_3PMo_{12}O_{40}$, albeit with a higher oxidation potential, than to $H_4PVMo_{11}O_{40}$. The catalytic oxidation chemistry supports this conclusion.

3. Conclusions

Phosphovanadomolybdates, $H_{3+x}PV_xMo_{12-x}O_{40}$ especially where $x = 1$ and 2, have unique and well-defined catalytic activity in electron transfer and electron transfer–oxygen transfer reactions. In an attempt to find yet more active catalysts, a new antimony(V) containing α-Keggin type acidic polyoxometalate, $H_4PSbMo_{11}O_{40}$, was prepared and characterized based on the assumption that compared to the well-known $H_4PVMo_{11}O_{40}$, $H_4PSbMo_{11}O_{40}$ would engender two-electron reactions at the antimony center and oxygen transfer would be facilitated by the lower electronegativity of Sb. Cyclic voltammetry showed that $H_4PSbMo_{11}O_{40}$ compound has a higher oxidation potential compared to the parent $H_3PMo_{12}O_{40}$, but catalytic activity was inferior to $H_4PVMo_{11}O_{40}$. In some cases no reactivity was observed, ET phenol oxidative dimerization and ET–OT sulfide, arene and alkylarene oxygenation. In other cases, dihydroarene aromatization and primary alcohol oxidation was observed, but the activity was lower than that of $H_4PVMo_{11}O_{40}$. DFT calculations show that $[PSbMo_{11}O_{40}]^{4-}$ is low spin as are the one and two-electron reduced compounds. The reduction of $[PSbMo_{11}O_{40}]^{4-}$ does not take place at the antimony atom as originally hypothesized. The first electron reduction occurs at a molybdenum center distal to the antimony atom while the two-electron reduction yields negative charge density quite delocalized over all molybdenum atoms.

4. Experimental

4.1. Synthesis of $H_4PSbMo_{11}O_{40}{\cdot}14H_2O$

$H_4PSbMo_{11}O_{40}{\cdot}14H_2O$ was synthesized by dissolving antimony(III) oxide (1.45 g, 5 mmol) in aqua regia (60 mL) on a hot plate at 70 °C to oxidize it to an antimony(V) species. This solution was

added to a solution of sodium phosphate (709.8 mg, 5 mmol) in 10 mL water. A drop of H_2SO_4 was added and the solution was stirred for 10 min at 70 °C then let cool to room temperature. Sodium molybdate dihydrate (12.1 g, 50 mmol) dissolved in 20 mL water was added. The color gradually changed from pale orange to clear yellow. The solution was further acidified by adding 8 mL HNO_3 dropwise and the solution was let to stir at room temperature for 15 h. The desired $H_4PSbMo_{11}O_{40}$ was extracted with diethyl ether to yield an etherate phase; the ether was then removed by evaporation. The crude mixture was dissolved in water and let to crystallize to give yellowish crystals with a green tint. Yield – 2.6 g (27%). Elemental Analysis $H_4PSbMo_{11}O_{40}{\cdot}14H_2O$ experimental (calculated) P: 1.11 (1.47), Sb: 5.53 (5.79), Mo: 49.78 (50.15) H_2O: 12.07 (11.87).

4.2. X-ray diffraction analyses

Crystal data for $H_4PSbMo_{11}O_{40}$ was measured at 100(2) K on a Bruker Kappa Apex2 CCD diffractometer [λ(Mo Kα) = 0.71073 Å] with a graphite monochromator. The data were processed with Apex2 software, respectively. The structures were solved by direct methods using the program SHELXS-97 and refined using SHELXL-97. All non-hydrogen atoms were refined anisotropically, using weighted full-matrix least squares on F^2 crystal data collection and refinement parameters are given in Table 1.

4.3. Other characterizations of $H_4PSbMo_{11}O_{40}$

The ^{31}P NMR spectra were measured in acetonitrile on a Bruker Avance DPX 300 spectrometer with H_3PO_4 as external standard. The IR spectra were measured on a Nicolet 6700 FTIR; samples were prepared as ~5 wt% KBr based pellets. Cyclic voltammetry was measured on CH Instruments, 680 Amp Booster model using glassy carbon working electrode and a platinum reference electrode. The UV/vis spectra were recorded on Agilent 89090A spectrophotometer using 0.3 mM solution in acetonitrile.

4.4. Catalytic oxidation reactions

Typically, oxidation reactions were carried out in 13 mL glass pressure tubes by loading the tube with appropriate amounts of the polyoxometalate, substrate and solvent. $H_4PSbMo_{11}O_{40}$ was treated with ozone prior to each reaction to ensure that all the catalyst is in its oxidized form. The tube was purged three times with the desired gas before loading it to 1 bar. The reaction tube was placed in a thermostated oil bath and the mixture stirred magnetically. Oxidation reaction products were characterized quantitatively and qualitatively using GC and GC/MS, respectively. The compounds were separated using a 30 m, 0.32 mm i.d. 5% phenyl methylsilicone column with a 0.25 mm coating using He as eluent.

4.5. DFT calculations

All calculations were performed with Gaussian 03 using the unrestricted UB3LYP density functional theoretic (DFT) method. Geometry optimization was performed with a Los Alamos-type LACVP basis set on Mo, Sb (with a small core ECP) and 6-31G on the rest of the atoms, henceforth, B1. Single point calculations were done using PCM model on B3LYP/B1 optimized geometries in two different solvents (water and acetonitrile) and single point B3LYP/Def2-TZVP calculations were also done on B3LYP/B1 optimized geometries i.e. B3LYP/B2D//B1.

Acknowledgement

This research was supported by the Israel Science Foundation grant # 1073/10 and the Helen and Martin Kimmel Center for Molecular Design. R. N. is the Rebecca and Israel Sieff Professor of Chemistry and D. K. is Ramanujan Fellow of the Department of Science and Technology (New Delhi, India).

Appendix A. Supplementary data

Supplementary data associated with this article can be found, in the online version, at doi:10.1016/j.molcata.2011.12.033.

References

[1] M.T. Pope, Heteropoly and Isopoly Oxometalates, Springer, Berlin, 1983.
[2] Catalysts for Fine Chemical Synthesis, Volume 2, Catalysis by Polyoxometalates, Kozhevnikov, I.V. Wiley, Weinheim, Germany, 2002.
[3] R. Neumann, M. Lissel, J. Org. Chem. 54 (1989) 4607–4610.
[4] R. Neumann, M. Levin, J. Org. Chem. 56 (1991) 5707–5710.
[5] M. Lissel, H. Jansen van de Wal, R. Neumann, Tetrahedron Lett. 33 (1992) 1795–1798.
[6] R. Neumann, M. Levin, J. Am. Chem. Soc. 114 (1992) 7278–7286.
[7] R. Neumann, I. Dror, Appl. Catal. A: Gen. 172 (1998) 67–72.
[8] A.M. Khenkin, I. Vigdergauz, R. Neumann, Chem. Eur. J. 6 (2000) 875–882.
[9] A.M. Khenkin, R. Neumann, Angew. Chem. Int. Ed. 39 (2000) 4088–4090.
[10] A.M. Khenkin, L. Weiner, Y. Wang, R. Neumann, J. Am. Chem. Soc. 123 (2001) 8531–8542.
[11] R. Ben-Daniel, R. Neumann, Angew. Chem. Int. Ed. 42 (2003) 92–95.
[12] R. Ben-Daniel, P. Alsters, R. Neumann, J. Org. Chem. 66 (2001) 8650–8653.
[13] O.V. Branytska, R. Neumann, J. Org. Chem. 68 (2003) 9510–9512.
[14] A.M. Khenkin, R. Neumann, J. Am. Chem. Soc. 126 (2004) 6356–6362.
[15] A.M. Khenkin, L. Weiner, R. Neumann, J. Am. Chem. Soc. 127 (2005) 9988–9989.
[16] O.V. Branytska, R. Neumann, Synlett (2005) 2525–2527.
[17] G. Maayan, B. Ganchegui, W. Leitner, R. Neumann, Chem. Commun. (2006) 2230–2232.
[18] R. Neumann, A.M. Khenkin, Chem. Commun. (2006) 2529–2538.
[19] A.M. Khenkin, R. Neumann, J. Am. Chem. Soc. 130 (2008) 14474–14476.
[20] H. Goldberg, I. Kaminker, D. Goldfarb, R. Neumann, Inorg. Chem. 48 (2009) 7947–7952.
[21] I. Kaminker, H. Goldberg, R. Neumann, D. Goldfarb, Chem. Eur. J. 16 (2010) 10014–10020.
[22] A.M. Khenkin, G. Leitus, R. Ronny Neumann, J. Am. Chem. Soc. 132 (2010) 11446–11448.
[23] A.M. Khenkin, R. Neumann, ChemSusChem 4 (2011) 346–348.
[24] F. Cavani, A. Tanguy, F. Trifirò, M. Koutrev, J. Catal. 174 (1998) 231–241.
[25] Y.-K. Lu, J.-N. Xu, X.-B. Cui, J. Jin, S.-Y. Shi, J.-Q. Xu, Inorg. Chem. Commun. 13 (2010) 46–49.
[26] L.H. Bi, E.B. Wang, R.D. Huang, C.W. Hu, J. Mol. Struct. 553 (2000) 167–174.
[27] M. Bösing, I. Loose, H. Pohlmann, B. Krebs, Chem. Eur. J. 3 (1997) 1232–1237.
[28] J. Fischer, L. Richard, R. Weiss, J. Am. Chem. Soc. 98 (1976) 3050–3052.
[29] I. Loose, E. Droste, M. Bösing, H. Pohlmann, M.H. Dickman, C. Rosu, M.T. Pope, B. Krebs, Inorg. Chem. 38 (1999) 2688–2694.
[30] U. Kortz, N.K. Al-Kassem, M.G. Savelieff, N.A.A. Kadi, M. Sadakane, Inorg. Chem. 40 (2001) 4742–4749.
[31] U. Kortz, M.G. Savelieff, B.S. Bassil, B. Keita, L. Nadjo, Inorg. Chem. 41 (2002) 783–789.
[32] L.J. Zhang, X.L. Zhao, J.Q. Xu, T.G. Wang, J. Chem. Soc., Dalton Trans. (2002) 3275–3276.
[33] X.X. Hu, J.Q. Xu, X.B. Cui, J.F. Song, T.G. Wang, Inorg. Chem. Commun. 7 (2003) 264–271.
[34] S.-Y. Shi, Y.-H. Sun, Y. Chen, J.-N. Xu, X.-B. Cui, Y. Wang, G.-W. Wang, G.-D. Yang, J.-Q. Xu, Dalton Trans. 39 (2010) 1389–1394.
[35] A.M. Khenkin, L.J.W. Shimon, R. Neumann, Eur. J. Inorg. Chem. 3 (2001) 789–794.
[36] U. Kortz, M.G. Savelieff, B.S. Bassil, M.H. Dickman, Angew. Chem. Int. Ed. 40 (2001) 3384–3386.
[37] U. Kortz, M.G. Savelieff, F.Y.A. Ghali, L.M. Khalil, S.A. Maalouf, D.I. Sinno, Angew. Chem. Int. Ed. 41 (2002) 4070–4073.
[38] Y.K. Lu, J.N. Xu, X.B. Cui, J. Jin, S.Y. Shi, J.Q. Xu, Inorg. Chem. Commun. 13 (2010) 46–49.
[39] R. Kiebach, C. Näther, W. Bensch, R. Kiebach, Solid State Sci. 8 (2006) 964–970.
[40] J.P. Wang, P.T. Ma, J.W. Zhao, J.Y. Niu, Inorg. Chem. Commun. 10 (2007) 523–526.
[41] J.P. Wang, P.T. Ma, J. Li, J.Y. Niu, Chem. Lett. 35 (2006) 994–995.
[42] W. Zhang, S.X. Liu, P. Sun, C.D. Zhang, F.J. Ma, D. Feng, J. Mol. Struct. 969 (2010) 76–80.
[43] W. Zhang, S.X. Liu, D. Feng, C.D. Zhang, P. Sun, F.J. Ma, J. Mol. Struct. 936 (2010) 194–198.
[44] S. Yao, Z.M. Zhang, Y.G. Li, E.B. Wang, Inorg. Chem. Commun. 12 (2009) 937–940.
[45] Y.-Y. Zhang, S.-X. Liu, C.-J. Yu, Q. Tang, D.D. Liang, C.D. Zhang, F.J. Ma, S.-J. Li, S.-W. Zhang, R.-K. Tan, Rui-Kang, Inorg. Chem. Commun. 13 (2010) 1418–1420.

[46] A. Ogawa, H. Yamato, U. Lee, H. Ichida, A. Kobayashi, Y. Sasaki, Acta Crystallogr. C44 (1988) 1879–1881.
[47] D. Drewes, G. Vollmer, B. Krebs, Z. Anorg. Allg. Chem. 630 (2004) 2573–2575.
[48] G.L. Xue, X.M. Liu, H.S. Xu, H.M. Hu, F. Fu, J.W. Wang, Inorg. Chem. 47 (2008) 2011–2016.
[49] Y.Z. Zhen, Q. Shen, L.L. Li, G.L. Xue, H.M. Hu, F. Fu, J.W. Wang, Inorg. Chem. Commun. 11 (2008) 886–888.
[50] G.A. Tsigdinos, C.J. Hallada, Inorg. Chem. 7 (1968) 437–441.
[51] H.T. Evans Jr., Perspect. Struct. Chem. 4 (1971) 1–59.
[52] H. Hirao, D. Kumar, H. Chen, R. Neumann, S. Shaik, J. Phys. Chem. C 111 (2007) 7711–7719.